Highly Oriented V_2O_5 Nanocrystalline Thin Films by Plasma-Enhanced Chemical Vapor Deposition

Davide Barreca,[†] Lidia Armelao,[†] Federico Caccavale,[‡] Vito Di Noto,[†] Andrea Gregori,[§] Gian Andrea Rizzi,[†] and Eugenio Tondello*[,†]

Centro di Studio sulla Stabilità e Reattività dei Composti di Coordinazione del CNR and Dipartimento di Chimica Inorganica, Metallorganica ed Analitica, Università di Padova, via Marzolo, 1-35131 Padova, Italy, or via Loredan, 4-35131 Padova, Italy; INFM and Dipartimento di Fisica, Università di Padova, via Marzolo, 8-35131 Padova, Italy; DTG, Università di Padova, Viale X Giugno, 22 36100 Vicenza, Italy

Received July 7, 1999. Revised Manuscript Received October 22, 1999

Plasma-enhanced chemical vapor deposition of vanadium pentoxide thin films from a vanadyl(IV) β-diketonate compound has been performed in a low-pressure reactor under different operating conditions. The effect of various parameters, such as the flow rates of the carrier and reactive gas and the substrate temperatures, on films composition, microstructure, and morphology was investigated in detail. Controlled variations of the synthesis conditions allowed a fine modulation of the sample properties, as shown by XRD and AFM analyses. In particular, at 200 °C and moderate oxygen flow, nanophasic V_2O_5 with a strong (001) preferential orientation could be easily obtained. The composition and purity of the films are studied by XPS and SIMS analyses, with special regard to film−substrate interdiffusion phenomena. Optical properties of the films are also investigated.

Introduction

The significant attention devoted to vanadium pentoxide thin films can be traced back to its interesting scientific and technological applications. In addition to its use in partial oxidation catalysis[1] and humidity sensors,[2] V_2O_5 has been widely studied as an electrochromic material[3] for the variability of its optical properties, that opens a broad perspectives of commercially attractive utilizations. For instance, V_2O_5-based systems have been proposed for variable transmission sunroofs, antiglare rearview mirrors, and surfaces with tunable emittance for temperature control of space vehicles.[4]

In recent years, the development of thin-film rechargeable batteries has attracted a great deal of interest due to their reduced resistivity with respect to bulk materials and to the possibility of incorporation into the same integrated circuit with other electronic elements.[5] In this context, V_2O_5-based thin layers offer important advantages, such as high charging capacity and extended cycling stability.[6] To this regard, nanophasic materials with a high active area are extremely interesting. Since the performances of the active layer are strongly dependent on the synthesis procedure, different techniques, such as RF-sputtering,[7] sol−gel,[8] and thermal evaporation,[9] have been applied to the preparation of vanadium oxide thin films. The different deposition methods and films characteristics for these systems have been recently reviewed.[3] Despite the various studies, however, further improvements in the films functional behavior are required and a deeper insight into the structure−properties relations is necessary to fully exploit the potential of these materials. A suitable choice of the synthesis procedure may in fact generate a better film morphology/structure with enhanced lifetime. A decrease of the deposition temperature would also help to stabilize the adjacent layers in the thin-film battery stack, avoiding the generation of a high thermal stress.

Plasma-enhanced chemical vapor deposition (PE-CVD), a versatile and efficient technique for large-area deposition of thin films, offers many of the advantages mentioned above. This technique takes advantage of the high-energy electrons present in glow discharges to dissociate and ionize gaseous molecules, thus generating chemically reactive radicals and ions. Film growth processes can be also modified by the presence of low-

* To whom correspondence should be addressed. E-Mail: Tondello@chim02.chin.unipd.it. Phone: 0039-49-8275220. Fax: 0039-49-8275161

[†] Centro di Studio sulla Stabilità e Reattività dei Composti di Coordinazione del CNR and Dipartimento di Chimica Inorganica, Metallorganica ed Analitica.

[‡] INFM and Dipartimento di Fisica.

[§] DTG.

(1) Ponzi, M.; Duschatzky, C.; Carrascull, A.; Ponzi, E. *Appl. Catal. A: General* **1998**, *169*, 373.

(2) Livage, J. *Chem. Mater.* **1991**, *3*, 758.

(3) Granquist, C. G. *Handbook of Inorganic Electrochromic Materials*; Elsevier Science: Amsterdam, 1995.

(4) Telledo, A.; Granquist, C. G. *J. Appl. Phys.* **1995**, *77*, 4655.

(5) Zhang, J.-G.; Liu, P.; Turner, J. A.; Tracy, C. E.; Benson, D. K. *J. Electrochem. Soc.* **1998**, *145*, 1889 and references therein.

(6) (a) Cazzanelli, E.; Mariotto, G.; Passerini, F.; Decker, F. *Solid State Ionics* **1994**, *70/71*, 412. (b) Park, H.-K.; Smyrl, W. H. *J. Electrochem. Soc.* **1995**, *142*, 1068. (c) Kuwabata, S.; Idzu, T.; Martin, C. R.; Yoneyama, H. *J. Electrochem. Soc.* **1998**, *145*, 2707. (d) Coustier, F.; Passerini, S.; Smyrl, W. H. *J. Electrochem. Soc.* **1998**, *145*, L73.

(7) For instance: Lourenco A.; Gorenstein, A.; Passerini, S.; Smyrl, W. H.; Fantini, M. C. A.; Tabacniks, M. H. *J. Electrochem. Soc.* **1998**, *145*, 706.

(8) Özer, N. *Thin Solid Films* **1997**, *305*, 80.

(9) Zhang, J.-G.; Mc Graw, J. M.; Turner, J.; Ginley, D. *J. Electrochem. Soc.* **1997**, *144*, 1630.

10.1021/cm991095a CCC: $19.00
Published on Web 12/15/1999

energy ion bombardment that assists the deposition. These events, which can cause preferential orientation of the growing films, allow very efficient depositions even at low temperatures with appreciable growth rates to be obtained,[10] resulting in material properties that may be unattainable with other processes.

The work presented here is the first part of a research program aimed at the realization of a V_2O_5-based thin-film rechargeable battery. The main goal of this paper is the development of a novel PE-CVD route to V_2O_5 thin films starting from a versatile precursor of formula $VO(hfa)_2 \cdot H_2O$ (Hhfa = 1,1,1,5,5,5-hexafluoro-2,4-pentanedione). We have recently used this compound to obtain by thermal CVD VO_2 rutile-type layers in an N_2 atmosphere, showing that the water molecule coordinated to the vanadium center favors the precursor decomposition in an inert atmosphere[11] as internal source of H^+ ions. However, the precursor decomposition in an O_2 atmosphere (the metal is oxidized from +4 to +5) was not very efficient and only very thin layers were obtained. In this work a PE-CVD route is used to overcome these limitation, thanks to the formation of reactive chemical species that greatly favor the precursor decomposition. In recent works, amorphous vanadium oxide films with variable stoichiometry from VO_2 to V_6O_{13} were obtained by RF reactive sputtering[7] and PE-CVD[12] using $VO(O^iPr)_3$ as precursor. In other PE-CVD syntheses, mixed phases were obtained;[5,13] however, the degree of crystallinity was low and the V_2O_5 phase was never obtained pure.

In the present study, single-phase nanocrystalline vanadium pentoxide films were obtained and the influences of various parameters (such as oxygen content and substrate temperature) on the composition, microstructure, and morphology of the layers are investigated in detail. The purpose of such analyses is 2-fold. First, a complete characterization of the chemicophysical properties of the material is a prerequisite for its practical applications. On the other hand, the correlation of film structure and properties with the deposition conditions provides important guidance for the optimization of the material to suit a given application. The depositions were carried out on borosilicate, glass, and surface-oxidized Si substrates in $Ar-O_2$ atmospheres at low temperatures. The microstructural features of the obtained samples were investigated by X-ray diffraction (XRD), while their surface and in-depth chemical composition were studied by X-ray photoelectron spectroscopy (XPS) and secondary ion mass spectrometry (SIMS). The surface morphology of the films was studied by atomic force microscopy (AFM) and their optical properties were also analyzed. Preliminary results have already been reported.[14]

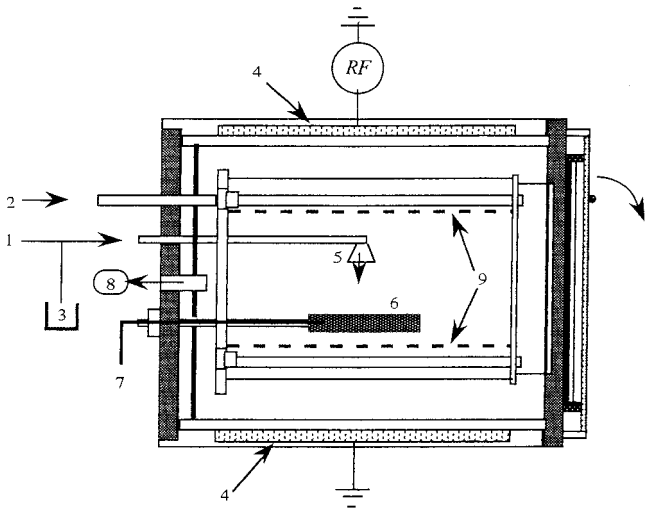

(1) Ar inlet
(2) Oxygen inlet
(3) Precursor reservoir
(4) Electrodes
(5) Injection nozzle for the precursor
(6) Susceptor
(7) Thermocouple
(8) Pumping system
(9) Faraday cage

Figure 1. Schematic diagram of the PE-CVD system with capacitively coupled RF power.

Experimental Section

The $VO(hfa)_2 \cdot H_2O$ complex was prepared according to the procedure reported by Selbin et al.[15] and its characterization has been reported elsewhere.[11]

Film Deposition. The films were deposited using a custom-built PE-CVD reaction system (Figure 1). The RF power (13.56 MHz, 300 W) was delivered to four electrodes capacitively coupled and surrounding a quartz reactor 18 cm in diameter. A metallic perforated cylindrical tube, acting as a Faraday cage, was inserted in the reactor to improve temperature and plasma uniformity. The substrate temperature was measured by a thermocouple inserted in the resistively heated sample holder. Electronic grade argon and oxygen were used as plasma sources. Oxygen was introduced in the reaction chamber through four perforated tubes, while a constant flow of argon (40 sccm) was used as the carrier gas. The precursor was placed in a vaporization vessel kept at 70 °C (evaporation rate $\approx 2 \times 10^{-4}$ mmol $m^{-2}s^{-1}$) and introduced in the reactor through an injection nozzle positioned above the substrates.

The barium borosilicate (Corning 7059) and soda-lime (Menzel-GL-C4SER) glass substrates were cleaned using a specific procedure for removing contaminants from glass surfaces which was recently developed in our laboratory. The slides were immersed in soaped water, washed with distilled water, and rinsed in isopropyl alcohol. After repeating this procedure several times, the substrates were dried in air and introduced in the reactor. Prior to V_2O_5 deposition, the substrates were subjected to a 10-min Ar plasma ion bombardment at 60 Pa and 300 W.

X-ray Diffraction. Diffraction patterns of thin film samples were recorded by a Philips diffractometer PW3710 using the Cu Kα radiation (λ = 1.54501 Å) and a proportional counter. The diffractometer was interfaced with a personal computer for controlling the measurements and storing the data.

XPS Analyses. A Perkin-Elmer Φ 5600ci spectrometer with monochromatized Al Kα radiation (1486.6 eV) was used for the XPS analyses. The working pressure was less than 1.8×10^{-9} mbar. The spectrometer was calibrated by assuming the binding energy (BE) of the Au $4f_{7/2}$ line at 83.9 eV with respect to the Fermi level with the use of a standard deviation of

(10) Hess, D. W.; Graves, D. B. In *Chemical Vapor Deposition: Principles and Applications*; Hitchman, M. L., Jensen, K. F., Eds.; Academic Press Inc.: London, 1993; p 397.
(11) Barreca, D.; Depero, L. E.; Franzato, E.; Rizzi, G. A.; Sangaletti, L.; Tondello, E.; Vettori, U. *J. Electrochem. Soc.* **1999**, *146*, 551.
(12) Spee, C. I. M. A.; Kirchner, G. In *Chemical Vapor Deposition*; Allendorf, M. D., Bernard, C., Eds.; Proceedings of the 14th International Conference and EUROCVD-11; The Electrochemical Society Proceedings Series: Pennington, NJ, 1997; PV 97-25, p 1490.
(13) Kuypers, A. D.; Spee, C. I. M. A.; Linden, J. L.; Kirchner, G.; Forsyth, J. F.; Mackor, A. *Surf. Coat. Technol.* **1995**, *74−75*, 1033.
(14) Barreca, D.; Battiston, G. A.; Caccavale, F.; Di Noto, V.; Gerbasi, R.; Gregori, A.; Rizzi, G. A.; Tiziani, A.; Tondello E. *J. Phys.* **1999**, *9*, 8−529.
(15) Selbin, J.; Maus, G.; Johnson, D. L. *J. Inorg. Nucl. Chem.* **1967**, *24*, 1735.

Table 1. Deposition Parameters and Thickness of V_2O_5 Films (See Experimental Section)[a]

sample	total P (Pa)	substrate T (°C)	oxygen flow rate (sccm)	thickness (nm)
1[b]	50	200	2.5	170
2[c]	58	200	5	130
3[c]	60	200	10	178
4[c]	70	200	20	175
5[b]	53	150	10	95
6[b]	55	290	10	105
7[b]	61	370	10	50

[a] Precursor temperature = 70 °C. Ar flow rate = 40 sccm. [b] Films deposited on glass substrates. [c] Films deposited on barium borosilicate substrates. The estimated uncertainty on the film thickness is ±15 nm.

0.10 eV. After a Shirley-type background subtraction, the raw spectra were fitted using a nonlinear least-squares fitting program adopting Gaussian−Lorentzian shapes for all the peaks. The atomic compositions were evaluated using sensitivity factors as provided by Φ V5.4A software. Depth profiles were carried out by Ar^+ sputtering at 2.5 kV, 0.4 μA cm^{-2} beam current density, and an argon partial pressure of 4×10^{-8} mbar.

SIMS Analyses. Depth profiles were obtained using a CAMECA IMS-4F ion microscope equipped with a normal incidence electron gun to compensate for charging effects. Depth profiles were obtained by 14.5 keV Cs^+ bombardment and negative secondary ion detection (beam current = 10 nA, raster area = 125×125 μm^2). After reaching the substrate, the thickness of the films was measured by an Alpha-Step 200 Tencor profilometer.

Optical Absorption. The vis−NIR absorption spectra of the films were recorded in transmittance mode at normal incidence on a Cary 5E (Varian) UV−vis−NIR spectrophotometer.

AFM Analysis. Images were taken using a Park Autoprobe CP instrument operating in contact mode in air. The micrographs were recorded in different areas of each sample, to test the film homogeneity. The background was subtracted from the images using the ProScan 1.3 software from Park Scientific.

Results and Discussion

The synthesis conditions and thickness of the films studied in the present work are reported in Table 1. To investigate the effect of the process parameters on the chemicophysical properties of the material, two sets of films have been prepared: in the first one (samples 1, 2, 3, and 4, set 1) the oxygen flow rate is varied at constant substrate temperature (200 °C), while in the second (samples 5, 3, 6, and 7, set 2) the effect of substrate temperature on the microstructure can be investigated.

All the films are yellow, homogeneous, and crack-free. Typical deposition rates are found in the range 1−2 nm/min, and showed limited dependence on the substrate temperature in the explored range. The thickness values, measured by the profilometer, are confirmed by an interferometric procedure as described in ref 16 for samples 2, 3, and 4. This analysis, however, proves to be unsuitable for the other films, since their optical spectra do not show interference fringes. For samples 1, 6, and 7 the fringes are probably hidden by d−d absorption of some V(IV), whose presence is confirmed by XPS analyses (see below).

Microstructural Characterization. Parts a and b of Figure 2 show the wide angle XRD patterns of the films formed at various oxygen flows and substrate temperatures. As can be seen, none of the films is amorphous, but the degree of crystallinity and orientation resulted dependent on the synthesis conditions. All the spectra are dominated by the intense peak located at $2\theta = 20.3°$, and, in some cases, another reflection at $2\theta = 40.4°$ appears. The peaks were indexed assuming the orthorhombic structure of V_2O_5 [17] and are assigned to the (001) and (002) planes, respectively. Since no other peaks were observed in the spectra, the films result highly textured with a very strong (001) preferential orientation. The appearance of the (00n) reflections suggests a regular stacking of imperfect *ab* planes,[18] that are built up of vanadyl oxygens.[19] This feature appears to be interesting for the use of the films as intercalation hosts for Li ions, like in reachargeable batteries and electrochromic devices.[20]

The structural analyses show that in our conditions a substrate temperature as low as 150 °C allows to grow a crystalline V_2O_5 film with a (001) preferential orientation. A similar texture has already been obtained,[21] but the crystallization temperatures were higher (from 170 to 240 °C).[22] In fact, the presence of low-energy particle bombardment, like in PECVD,[10] can either lower the crystallization temperature or induce preferred orientation.

The mean crystallites size was calculated by applying the Debye−Scherrer equation to the most intense (001) peak. The obtained values range from 14 nm for sample 7 to 30 nm for sample 4, indicating that all the films in Table 1 are nanostructured. As outlined in the Introduction, this feature is particularly interesting for applications of the films that require a high active area, such as in reachargeable batteries, since nanophasic materials are mostly formed of interfacial regions.[23]

On going from sample 1 to 2, i.e. on increasing the oxygen flow rate from 2.5 to 5 sccm, the nanocrystallites size increases from 17 to 29 nm and the (001) peak becomes much more intense. Correspondingly, the (002) peak appears, indicating a higher degree of crystallinity and preferred orientation. In fact, the oxygen content used in the synthesis of sample 1 is probably too low to oxidize all the V(IV) present in the precursor (see XPS analyses) and lead to the formation of pure and well-crystallized V_2O_5. On increasing oxygen flow rate to 20 sccm (sample 4), the intensity of the (002) peak decreases again, indicating a lower degree of crystallinity. This *plateau* effect indicates that the optimal conditions for the growth of nanocrystalline V_2O_5 films

(16) Swanepoel, R. *J. Phys. E: Sci. Instrum.* **1983**, *16*, 1214.

(17) *Inorganic Crystal Structure Database*; ICSD: Karlsruhe, Jan 1997; card no. 60767.

(18) Audiere, J. P.; Madi, A.; Grenet, J. C. *J. Mater. Sci.* **1982**, *17*, 2973.

(19) Smith, L. R.; Rohrer, G. S.; Lee, K. S.; Seo, D.-K.; Whangboo, M.-H. *Surf. Sci.* **1996**, *367*, 87.

(20) (a) Park, H.-K.; Smyrl, W. H. *J. Electrochem. Soc.* **1994**, *141*, L25. (b) Lakshmi, B. B.; Patrissi, C. J.; Martin, C. R. *Chem. Mater.* **1997**, *9*, 2544.

(21) (a) Shimizu, Y.; Nagase, K.; Miura, N.; Yamazoe, N. *Jpn. J. Appl. Phys.* **1990**, *29*, L1708. (b) Abo El Soud, A. M.; Mansour, B.; Soliman, L. I. *Thin Solid Films* **1994**, *247*, 140.

(22) (a) Kobayashi, S.; Takenura, T.; Kaneko, F. *Jpn. J. Appl. Phys.* **1987**, *26*, L1274. (b) Szörényi, T.; Bali, K.; Hevesi, I. *J. Non-Cryst. Solids* **1980**, *35*−*36*, 1245.

(23) Yu, K. N.; Xiong, Y.; Liu, Y.; Xiong, C. *Phys. Rev. B* **1997**, *55*, 2666.

Table 2. XPS Data Obtained Form the Surface Analysis of the As-Grown Films[b]

sample	V2p$_{3/2}$(I) (eV) (%)	V2p$_{3/2}$(II) (eV) (%)	ΔBE(O1s(I) − V2p$_{3/2}$) (eV)[a]	O/V
1	517.4 (54.9)	516.3 (45.1)	12.9	2.6
2	517.3	*b*	12.8	2.3
3	517.2	*b*	12.8	2.4
4	517.3	*b*	12.8	2.4
5	517.2	*b*	13.0	2.4
6	517.2 (89.6)	516.0 (10.4)	13.0	2.4
7	517.3 (86.1)	516.1 (13.9)	13.0	2.4

[a] BE difference between the oxide component of the O 1s peak and the component I of the V2p$_{3/2}$ peak. [b] Component is not detected.

with a strong preferred orientation require intermediate O_2 flow rates (∼10 sccm).

A similar behavior is observed for the second set of samples (5, 3, 6, and 7). On increasing the temperature from 150 to 370 °C, the intensity of the diffraction peaks is first enhanced and then undergoes a sharper decrease than that observed on increasing oxygen flow rate. This effect can be attributed to a decrease of the film thickness (see Table 1), due to gas-phase reactions depleting the V-precursor flow arriving at the surface at temperatures greater than 200 °C. In fact, as shown in a previous study,[11] heat treatments of the precursor at T > 200 °C lead to the formation of the geminal diole $CF_3COCH_2C(OH)_2CF_3$, through the nucleophilic attack of a water molecule to the ligand. A temperature increase favors the formation of this product, which might subsequently evolve to the dicarbonylic compound. In any case, this effect can be considered the main cause for the precursor depletion at temperatures higher than 200 °C. We also think that a contribution of the bombarding effect previously discussed cannot be completely excluded.

XPS Analyses. The composition and purity of the obtained layers are studied by surface and in-depth XPS. No surface charging is ever detected, in accordance with the *n*-type semiconductor character of V_2O_5.[24] Only vanadium, oxygen, and carbon are found in the films. Since the presence of fluorine, which is directly bonded to carbon in the precursor, is never observed, we are induced to suppose that volatile fluorinated byproducts are eliminated in the precursor thermal decomposition. A similar behavior has been previously observed in the thermal CVD of vanadium oxides from the same precursor.[11]

The data obtained from the analysis of the surface photoelectron peaks are reported in Table 2. V2p$_{3/2}$ peak can be fitted with a single component, except for samples 1, 6, and 7. This component has a BE which ranges from 517.2 to 517.4 eV, in accordance with literature data for V_2O_5.[8,25] In addition to the V(V) component, samples 1, 6, and 7 show the presence of a smaller peak centered at about 516.1 eV (see Figure 3 for sample 6), whose BE can be attributed to the existence of V(IV) oxides.[25] In the case of sample 1 their presence, which is not detected from XRD analyses, is probably due to an incomplete oxidation of the precursor. In fact, as already observed in the previous section, the oxygen content used for its deposition is very low. In the case of sample 6 and 7, the V(IV) species might arise from a different decomposition mechanism of the precursor compound, due to a more effective formation of $CF_3COCH_2C(OH)_2CF_3$ at temperatures higher than 200 °C (see the Microstructural Characterization section).

The O/V surface ratio for the films (Table 2) is always greater than two, indicating a possible adsorption of other species due to the interaction with the outer atmosphere. Indeed, the surface O 1s peak shows the presence of two components. The first one, at about 530.3 eV, is due to the oxide species,[8,25,26] while the second, located at 531.3−531.5 eV, can be attributed to some unspecified surface contaminant. The disappearance of this component after a mild sputtering indicates that the corresponding species arise from interactions with the outer atmosphere and do not originate from the decomposition of the precursor compound. This observation proves that even in the plasma environment the water molecule coordinated to vanadium in the precursor is completely consumed through the nucleophilic attack to the β-diketonate ligands.[11] In each case, the presence of V_2O_5 as the main phase is confirmed by the BE differences between V2p$_{3/2}$(I) peak and the oxide component of the O 1s peak (∼13 eV, see Table 2), which are in good agreement with the value reported for vanadium pentoxide.[27]

Depth profiles give similar results for all the obtained samples. The carbon percentage falls below 1 atom % after a mild sputtering, indicating that no undecomposed precursor is present in the oxide matrix. After erosion for 1 min, the O/V ratio becomes lower than 2 because of oxygen preferential sputtering;[28] however, the films result to be homogeneous and pure, since O and V percentages remain constant from the outermost layers up to the substrate interface. Here a certain interdiffusion of the oxide moieties into the glass matrix was observed, as confirmed by SIMS analyses (see below).

In-Depth SIMS Analyses. SIMS depth profiles are carried out on different areas of each samples to test their homogeneity. The values for film thickness (Table 1) are measured at the end of each profile by measuring the depth of the crater through a profilometer. Although the thickness results to be dependent on the synthesis conditions, the ion profiles are qualitatively similar for all the films.

Figure 4 reports the depth profiles of O, V, and Na for sample 1, deposited on soda-lime glass. It is worth noting the existence of an outer region (A) where vanadium and oxygen ion yields are lower than in the inner part of the films (B). The A region, whose presence was detected for all the analyzed samples, is about 50 nm thick and for sample 7 corresponds to the entire deposit. The ion yields increase on going from A to B

(24) Shin, S.; Suga, S.; Taniguchi, M.; Fujisawa, M.; Kanzaki, H.; Fujimori, A.; Daimon, H.; Ueda, Y.; Kosuge, K.; Kachi, S. *Phys. Rev. B* **1990**, *41*, 4993.

(25) Mendialdua, J.; Casanova, Y.; Barbaux, Y. *J. Electron Spectrosc. Relat. Phenom.* **1995**, *71*, 249.

(26) (a) Nefedov, V. I.; Gati, D.; Dzhurinskii, B. F.; Sergushin, N. P.; Salyn', Ya. V. *Zh. Neorg. Khim.* **1975**, *20*, 2307. (b) Sawatzky, G. A.; Post, D. *Phys. Rev. B* **1979**, *20*, 1546.

(27) (a) Fujita, Y.; Miyazaki, K.; Tatsuyama, C. *Jpn. J. Appl. Phys.* **1985**, *24*, 1082. (b) Khan, G. A.; Hogarth, C. A. *J. Mater. Sci.* **1991**, *26*, 597.

(28) Briggs, D.; Seah, M. P. In *Practical Surface Analysis by Auger and X-ray Photoelectron Spectroscopy*; J. Wiley & Sons: Chicester, UK, 1988.

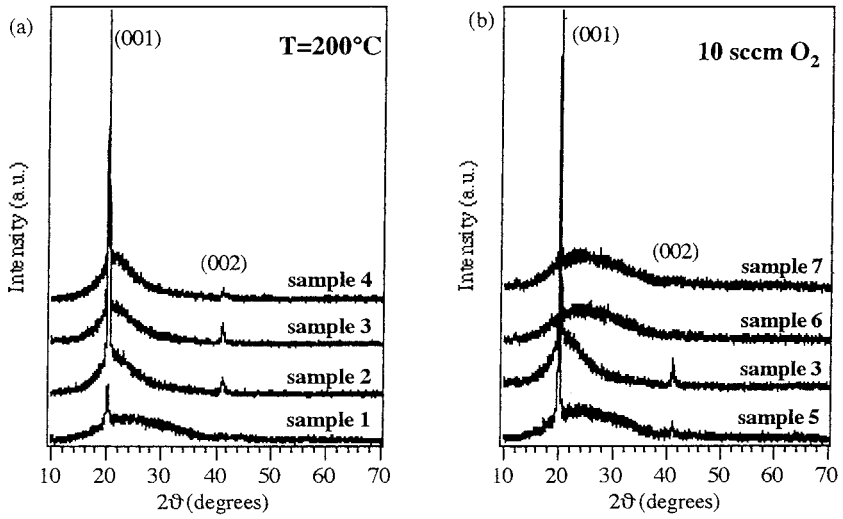

Figure 2. X-ray diffraction patterns of the obtained samples: (a) set 1 (constant substrate temperature) and (b) set 2 (constant oxygen flow rate).

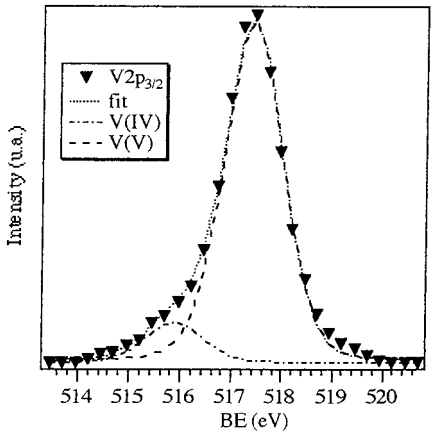

Figure 3. Deconvolution of the XPS $V2p_{3/2}$ surface peak for sample 6. The low binding energy component corresponding to V(IV) is clearly evident.

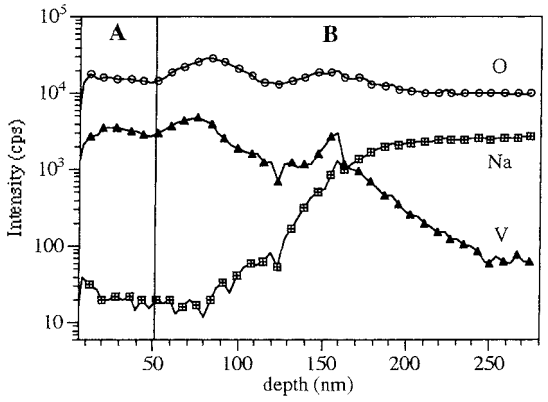

Figure 4. SIMS depth profile of sample 1, supported on soda-lime glass.

can be correlated with an increase in density of the oxide matrix. On the basis of the structural analysis, such an effect is attributable to ion bombardment by the impinging particles that are present in the plasma atmosphere. Although the thickness of the region subjected to this effect is almost equal for all the films because the discharge conditions are the same (see Experimental Section), an increase in the oxygen content (sample set 1) causes a more pronounced ion bombardment effect and a decrease in crystallinity. For sample 5, 6, and 7, that are thinner than films belonging to set 1, region A corresponds to a greater portion of the total thickness. This effect might contribute to their lower crystallinity and decreased preferential orientation (see Figure 2).

SIMS data indicate that the films resulted to have a quite homogeneous composition, since both oxygen and vanadium ion yields are almost constant on going from the film to the substrate interface. Film−substrate interdiffusion phenomena, which probably originate during the film deposition, can be clearly observed from Figure 4. Since neither the thickness of the films nor the ion profiles shapes show appreciable changes after annealing the samples at 300 °C in air for 3 h, it is reasonable to suppose that interdiffusion effects are strongly influenced by the presence of low-energy particle bombardment during the film growth.[10]

Optical Absorption. The optical transmission spectra of vanadium pentoxide thin films (not shown) are similar to those previously reported.[7,21b] A relatively high transmission for wavelengths greater than 600 nm indicates that the films are weakly absorbing in this range. In the spectra of samples 1, 6, and 7 the d−d transitions of V(IV) centers[29] are detected for $\lambda > 600$ nm. These transitions are typically broad, probably due to the presence of V(IV) in slightly different octahedral environments, and extend up to 2000 nm, so that interference fringes are completely hidden. The presence of V(IV) only in these three samples is in agreement with the XPS analyses (see Table 2).

The refractive index $n(\lambda)$, evaluated as reported in ref 16, ranged from 2.3 to 2.6 for each of the analyzed samples, in accordance with literature data.[30] The optical absorption coefficient α of the films is calculated using the relation:[31]

$$\alpha t = \ln(T^{-1}) \qquad (1)$$

where T is the trasmittance and t is the film thickness.

(29) Bullot, J.; Cordier, P.; Gallais, O.; Gauthier, M.; Babonneau, F. *J. Non-Cryst. Solids* **1984**, *68*, 135.
(30) Ramana, C. V.; Hussain, O. M.; Uthanna, S.; Srinivasulu Naidu, B. *Opt. Mater.* **1998**, *10*, 101.
(31) Varma, S.; Rao, K. V.; Kar, S. *Chemtronics* **1986**, *1*, 61.

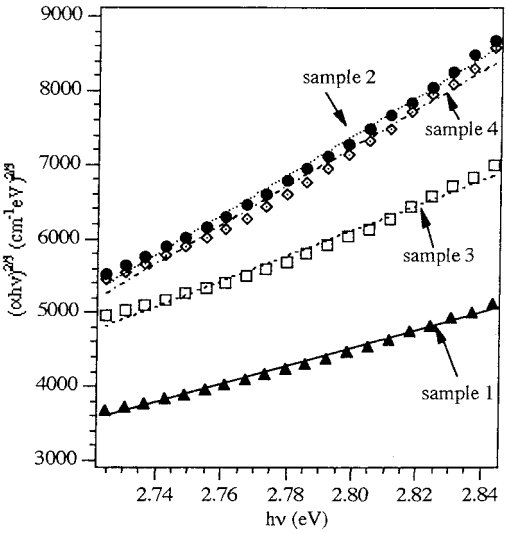

Figure 5. $(\alpha h\nu)^{2/3}$ vs $h\nu$ plots for vanadium pentoxide thin films belonging to set 1.

In the high absorption region (λ < 500 nm) the optical absorption follows a power law of the form:

$$\alpha(h\nu) \propto (h\nu - E_G)^n \qquad (2)$$

where E_G is the band gap and n is an exponent that can have different values depending on the nature of the electronic transition. It has been recently shown that for vanadium pentoxide $n = {}^3/_2$ for λ < 500 nm, corresponding to direct forbidden transitions.[30] Figure 5 shows the plots of $(\alpha h\nu)^{2/3}$ vs $h\nu$ for vanadium pentoxide thin films deposited with different oxygen flow rates, at constant substrate temperature (set 1). The optical band gaps for the films, which were evaluated by extrapolating the linear plots to zero (i.e., $\alpha = 0$), are all very close to 2.4 eV, irrespective of the oxygen flow rate. Ramana and co-workers[30] have reported a variation of the energy gap in electron-beam evaporated V_2O_5 films from 2.04 to 2.30 eV on increasing oxygen partial pressure from 10^{-7} to 10^{-4} mbar. Since in the present case the variation in $p(O_2)$ are much smaller, the fact that E_G is almost constant is not unexpected. Our band gap data are in good agreement with those reported by several authors for bulk and thin films V_2O_5, that range from 2.1 to 2.6 eV depending on the synthesis conditions.[7,21b,29,30] Similar results were obtained for the samples deposited at different substrate temperatures (set 2; graphs not reported).

Morphology. The dependence of the morphological features on the synthesis conditions was investigated by AFM surface analysis of the different V_2O_5 films. All the samples show a smooth surface, with a fine texture characterized by small particles well interconnected among themselves.

The AFM images of films belonging to set 1 indicate that on going from sample 1 to 4, i.e. on increasing oxygen flow rate, the average particle size becomes bigger and the surface more rough; indeed, the average roughness increases from 6 to 7.5 nm. The increase of the average roughness might be due to a more extensive bombarding effect at higher oxygen content, as explained in the Microstructural Characterization section. It is interesting to observe that the mean particle sizes show an almost linear increase either on increasing the O_2 flow rate (sample set 1) or on increasing the deposition temperature (sample set 2, Figure 6). This indicates an evolution of the morphology as a function of the substrate temperature or of the oxygen content, the other conditions being constant. Therefore, the morphological features of the samples can be suitably tailored by an adequate choice of the synthesis conditions.

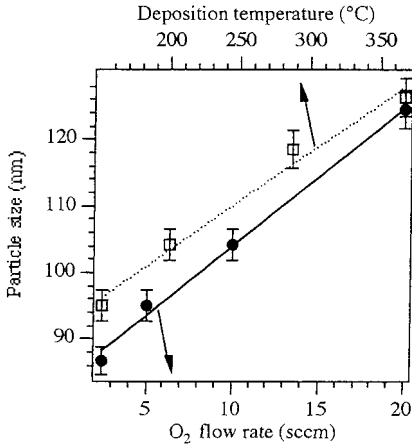

Figure 6. Dependence of AFM grain size on the oxygen flow rate (sample set 1) and on the substrate temperature (sample set 2). The continuous lines were obtained by fitting the experimental data with linear curves.

Conclusions

Pure V_2O_5 nanocrystalline thin films were successfully deposited via PE-CVD using $VO(hfa)_2 \cdot H_2O$ as precursor, at temperatures as low as 150 °C. The samples show a well-defined (001) preferential orientation strongly dependent on the synthesis conditions. In particular, the optimal conditions to obtain nanocrystalline and oriented V_2O_5 films result from an equilibrium between the film growth and the ion bombardment produced by gaseous species in the plasma environment. The presence of an ordered microstructure opens intriguing perspectives for the use of the layers as intercalation hosts for Li^+ or Mg^{2+} ions in thin-film rechargeable batteries.

The use of different analytical techniques allowed us to gain a complete characterization of the chemicophysical properties of the films. As shown by XRD and AFM analysis, the microstructural and morphological features of the films can be suitably tailored by a proper choice of the deposition conditions. XPS and SIMS investigations indicate that the films composition is homogeneous. The optical absorption spectra confirm that all the analyzed films are mainly composed by V_2O_5, irrespective of the process parameters. A systematic analysis of the conduction properties of the different V_2O_5 films in order to identify the optimal synthesis conditions for a thin-film rechargeable battery is in progress.

Acknowledgment. The authors are grateful to Dr. G.A. Battiston and Dr. R. Gerbasi (ICTIMA-CNR, Padova, Italy) for useful discussions and technical assistance.

CM991095A